

Article

# Inhomogeneous Superconductivity in Organic and Related Superconductors

Charles C. Agosta 

Department of Physics, Clark University, 950 Main Street, Worcester, MA 01610, USA; cagosta@clarku.edu

Received: 16 May 2018; Accepted: 24 June 2018; Published: 11 July 2018



**Abstract:** Evidence of inhomogeneous superconductivity, in this case superconductivity with a spatially modulated superconducting order parameter, has now been found in many materials and by many measurement methods. Although the evidence is strong, it is circumstantial in the organic superconductors, scant in the pnictides, and complex in the heavy Fermions. However, it is clear some form of exotic superconductivity exists at high fields and low temperatures in many electronically anisotropic superconductors. The evidence is reviewed in this article, and examples of similar measurements are compared across different families of superconductors. An effort is made to find a consistent way to measure the superconducting energy gap across all materials, and use this value to predict the Clogston–Chandrasakhar paramagnetic limit  $H_p$ . Methods for predicting the existence of inhomogeneous superconductivity are shown to work for the organic superconductors, and then used to suggest new materials to study.

**Keywords:** organic superconductors; inhomogeneous superconductors; FFLO; quasi 2D materials

## 1. Introduction

It is becoming evident that an exotic superconducting phase, associated with inhomogeneous superconductivity, has been realized in a number of organic conductors, and possibly in a pnictide superconductor as well. In this chapter, we will compare experimental evidence that supports the discovery of Fulde, Ferrell, Larkin, Ovchinnikov (FFLO) states, and examine methods to search for new materials where a FFLO state could be stabilized.

The most compelling evidence for the FFLO state comes from systematic measurements of quasi-two-dimensional organic superconductors that suggest that an inhomogeneous superconducting state can be stabilized if a magnetic field is applied precisely parallel to the conducting layers. This exotic superconducting state, a tunable mixture of a spatially modulated superconducting order parameter and a magnetic lattice created by the remaining unpaired electrons, was predicted over 50 years ago, and is called the FFLO state after the authors Fulde, Ferrell, Larkin, and Ovchinnikov, who first predicted it [1,2]. The topology of the FFLO state enhances the stability of the superconducting state, and allows superconductivity to survive at higher magnetic fields than what is predicted from the size of the superconducting energy gap. It only exists when orbital effects, manifested as vortices in superconductors, can be suppressed, and an advantage of anisotropic superconductors is that they can be studied with or without the effects of vortices, by aligning the magnetic field perpendicular or parallel to the conducting planes, respectively. The FFLO state is highly tunable via temperature, the direction and strength of the magnetic field, and pressure. It is sensitive to impurity scattering and a magnetic scattering process called spin-orbit scattering, an effect that magnetically spin flips itinerant electrons. These attributes make it a rich system for the study of correlated electrons, and, in particular, superconductivity. Many of the details of the FFLO state will be discussed below with references. The discussion will focus on organic superconductors where the evidence for the FFLO state is more compelling, although pnictides and heavy Fermions will be addressed briefly.

A sampling of the best recent evidence for the FFLO state comes from the following measurements of organic superconductors:

- $\kappa$ -(BEDT-TTF)<sub>2</sub>Cu(NCS)<sub>2</sub>, specific heat [3], torque magnetometry [4,5], rf penetration depth [6], resistivity [5], NMR [7,8],
- $\lambda$ -(BETS)<sub>2</sub>GaCl<sub>4</sub> thermal conductivity [9], rf penetration depth [10],
- $\beta''$ -(ET)<sub>2</sub>SF<sub>5</sub>CH<sub>2</sub>CF<sub>2</sub>SO<sub>3</sub> rf penetration depth [11], NMR [12].

For the rest of this manuscript, we will use these abbreviations for the following compounds:

- $\kappa$ -(BEDT-TTF)<sub>2</sub>Cu(NCS)<sub>2</sub>: $\kappa$ ET-CuNCS,
- $\lambda$ -(BETS)<sub>2</sub>GaCl<sub>4</sub>: $\lambda$ BETS-GaCl,
- $\beta''$ -(ET)<sub>2</sub>SF<sub>5</sub>CH<sub>2</sub>CF<sub>2</sub>SO<sub>3</sub>: $\beta''$ ET-SF5,
- $\kappa$ -(ET)<sub>2</sub>Cu[N(CN)<sub>2</sub>]Br: $\kappa$ ET-Br.

Given the number of materials now showing evidence of the FFLO state, and the wide variety of measurement techniques available to investigate the details of the FFLO state, the prospect of learning new fundamental facts about the microscopic mechanisms of superconductivity is compelling. For example, as detailed measurements of the FFLO state have become available, comparison between theory, particularly early theory [13–19], and experiments (see references throughout the article) are finally possible. Certain results have been consistent with theory, such as the first order nature of the vortex state to the FFLO state phase line [3,20], but other aspects of the FFLO state, such as the onset temperature,  $T^*$ , are not consistent with prevailing theory [17]. After a brief description of inhomogeneous superconductivity, the results of experiments that have been done to date will be reviewed to see how well the results match each other, and with what is expected from the theory of inhomogeneous superconductivity. In addition, tests will be described to determine if a superconductor is a candidate for inhomogeneous superconductivity. This analysis will begin to determine if the proposed FFLO states that have been discovered are universal, or specific to each material.

These studies are important for the basic and applied understanding of materials. As an example, superconductivity is sometimes related to the existence of a quantum critical point, and a quantum critical point may be an important signature of the FFLO state [21]. The FFLO state has also been studied, at least theoretically, in cold atom systems, and attempts have been made to create model systems to study FFLO interactions with highly tunable parameters [22–27]. On the more practical side, the understanding of correlated electron states in new materials is not only the basis of understanding phenomena such as superconductivity, but it is also the starting point for developing new electronic devices, many which will be based on magnetic properties. The FFLO superconducting state will further the understanding of the relationship between superconductivity and magnetism. Magnetism is now recognized as one of the key drivers of superconductivity, but the exact nature of the mechanism that lets magnetism drive superconductivity is not known (see, for instance, these reviews [28,29]). The interplay of magnetism and superconductivity is critical to the understanding of most superconductors of interest, including metallic, cuprate, and iron based pnictide materials.

### 1.1. Inhomogeneous Superconductivity

In order to understand the genesis of inhomogeneous superconductivity, it is important to understand what suppresses superconductivity. In most cases, superconductivity is destroyed in an external magnetic field due to vortices—non-superconducting regions containing a magnetic field line shielded by circulating Cooper pairs—which increase in density as the magnetic field is increased and ultimately displace the superconducting phase. Chandrasekhar [30] and, independently, Clogston [31] were the first to recognize that, if the formation of vortices could be suppressed, superconductivity could persist only to a magnetic field limit determined by the Pauli paramagnetism of the electrons denoted as  $H_P$ , and properly called the Chandrasekhar–Clogston Pauli paramagnetic limit [32]. We will refer to this level of magnetic field as the paramagnetic limit for short.

At this magnetic field, the energy to flip an electron spin between the up and down states, the Zeeman energy  $\mu_b H$  exceeds the binding energy of the Cooper pairs, destroying the pairs. Soon after the Chandrasekhar and Clogston papers, it was found that the upper critical field of a superconductor in the paramagnetic limit changes from a continuous to a first-order transition below  $t = T/T_c \sim 0.5$  [33,34]. After further study, it was proposed that, if Pauli paramagnetism was the dominant cause for limiting superconductivity and the superconductor was clean ( $r > 1$ , where  $r = \ell/\xi$  and  $\ell$  is the mean free path of the quasiparticles and  $\xi$  is the superconducting coherence length), a new kind of superconducting state could be stabilized at a magnetic field above  $H_p$ . This new superconducting state is the FFLO state and is characterized by Cooper pairs with non-zero momentum, and a spatially modulated order parameter [1,2].

A diagram of this modified electron pairing is shown in Figure 1, reproduced from a recent article by Wosnitza [35]. A momentum  $\mathbf{q}$  is added to one of the  $\mathbf{k}$  vectors (electrons) to compensate for the energy difference in a magnetic field between the up and down spins, which creates an electron with non-zero momentum, but a Cooper pair with a center of mass momentum of zero. As described in the figure caption, in real material, more complex diagrams could exist. The Fermi surface could create a preferential direction for  $\mathbf{q}$ , creating a modulated order parameter in one dimension, or a set of  $\mathbf{q}$  vectors creating a two- or three-dimensional modulation of the order parameter [15,16,20]. In particular, it is shown that, in higher magnetic fields, more complex combinations of  $\mathbf{q}$ -vectors form more complicated, higher dimensional order parameter patterns. In Figure 2, a cartoon taken from Agosta et al. [3], shows a simple real space model of a FFLO state with the  $\mathbf{q}$ -vector aligned with the applied magnetic field. In a real, highly anisotropic organic superconductor as suggested by the discussion of Figure 1, the  $\mathbf{q}$ -vector could also align in another direction in the conducting plane, for example perpendicular to the magnetic field, as determined by the anisotropic Fermi surface and as depicted in Figure 5b from Mayaffre et al. [8]. The influence of the Fermi surface on the stability and the details of a FFLO state are discussed in a number of papers [36–40], including how an elliptical Fermi surface can improve the stability of the FFLO state [35]. Other symmetry breaking properties of the material such as the crystal anisotropies or the symmetry of the Cooper pair wave function could also influence the  $\mathbf{q}$ -vector, as described in many studies [13,15,16,20,38,41,42]. As suggested above, the greatest influence on  $\mathbf{q}$  in the organic superconductors is probably the shape of the Fermi surface, particularly if the closed pockets are highly elliptical [35].

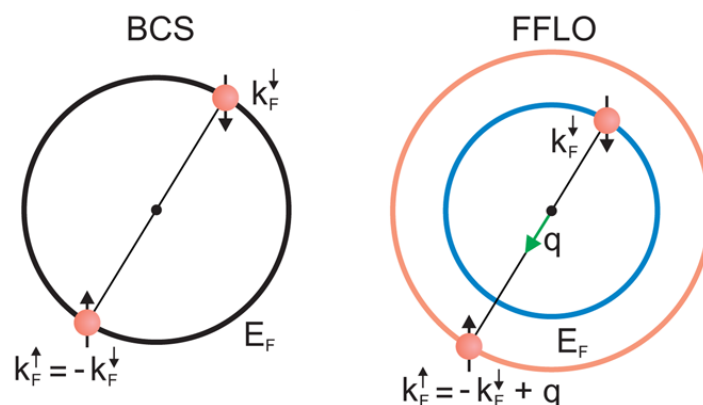


**Figure 1.** Color online. From Wosnitza [35] On the left, the traditional BCS Cooper pair is represented. On the right, the energy of the up and down electrons have been shifted by the magnetic field. A momentum  $\mathbf{q}$  can be added to one of the electrons to create a zero momentum center of mass Cooper pair. In the diagram, the initial momentum of the electrons is isotropic. In real material, the shape of the Fermi surface could create more complex diagrams.

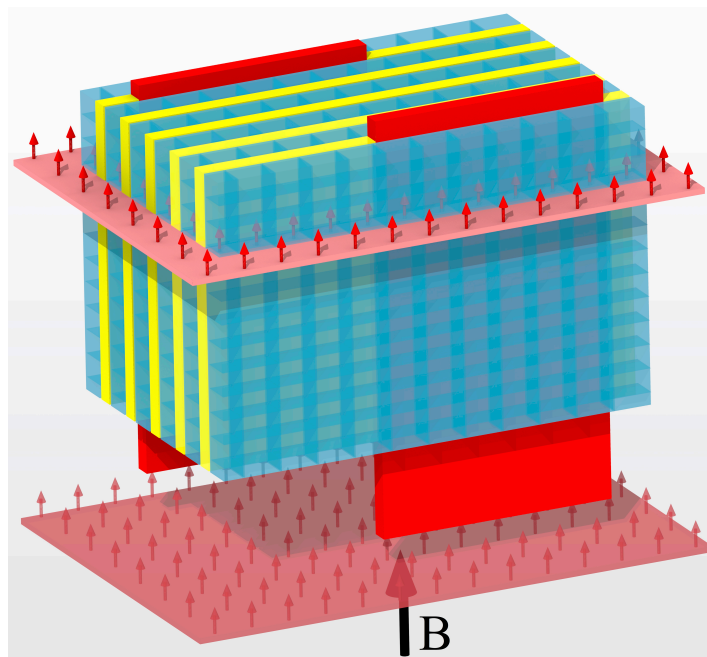


**Figure 2.** Color online, from [3]. Cartoon of the FFLO state showing the nodes in the order parameter as horizontal planes where we estimate the spin-polarization to be  $\approx 10\%$  at 25 T in the low temperature limit. In the diagram the black arrow labeled **B** represents the applied magnetic field, and the red arrows represent the net spin polarization. Although the diagram is schematic, all of the lengths are to scale; small boxes represent the unit cells of  $\kappa$ ET-CuNCS, yellow slabs represent the least conducting layers of the crystal, and red rectangles represent Josephson core-less vortices at about the right distance apart in a 25 T field. The full height of the crystal is  $\approx 20$  nm.

As another example of the effect of the crystal anisotropy, observe that the vortices depicted in Figure 2 are highly elongated Josephson vortices. This is due to the difficulty of driving super-currents perpendicular to the conducting planes in a highly anisotropic superconductor such as the crystalline organics where the layers are Josephson coupled. The perpendicular current density is limited to the value of the Josephson tunneling current density, and the vortex needs to elongate to find enough surface area to have equal current along the superconducting planes as there exists across the quasi-insulating layers, to form the vortex. The existence of inhomogeneous superconductivity in highly 2D Josephson coupled layered superconductors was treated early on, before the discovery of organic superconductors, by Bulaevskii [43]. There is no doubt that Josephson coupling exists in organic conductors, as it has been measured indirectly [44,45] as well as being imaged directly [46]. Furthermore, in a recent calculation, it is shown that, in these highly anisotropic organic superconductors, orbital currents are confined to just one layer [47].

### 1.2. Critical Parameters

Ideally, one should be able to measure a few critical parameters that will indicate if a material is in the paramagnetic limit at low temperatures or, in more interesting cases, has a FFLO or related inhomogeneous superconducting state. One of two parameters that are useful for this purpose is the Maki parameter

$$\alpha_M = \sqrt{2}H_{orb}^0/H_P, \quad (1)$$

where

$$H_{orb}^0 = 0.7T_c \left. \frac{dH_{c2}}{dT} \right|_{T_c}, \quad (2)$$

the orbital critical field at zero temperature [48], is the critical field as if there were no spin-paramagnetic pair breaking, just vortices. This formula was derived for 3D isotropic superconductors, and, for 2D materials, the more complicated results in Klemm et al. [32] or Schneider et al. [49] should be used; however for a simple comparison of the anisotropy between materials, the  $H_{c2}$  slope near  $T_c$  is valid. In addition, many superconductors of recent interest are two gap, or multiband superconductors, and additional theories exist for those materials [42]. Therefore, a large Maki parameter  $\alpha_M$  suggests that the orbital pair breaking happens at a higher field than  $H_P$ , and Pauli paramagnetism will dominate, favoring inhomogeneous superconductivity. The other parameter  $r$ , defined above, is a measure of how clean the system is. It measures the ability for the material to support an extended wave function, necessary for the long range order of the FFLO state [39], although there are claims that clean ordered systems are not absolutely necessary [50]. These parameters come from routine measurements. In the ratio  $r = \ell/\xi$ ,  $\ell$  comes from the scattering time, which is related to the Dingle temperature,  $T_D$ , and the Fermi velocity,  $v_F = \sqrt{2E_F/m^*}$ , where  $E_F$  is the Fermi energy and  $m^*$  is the effective mass. The Fermi energy, effective mass, and  $T_D$ , can all be measured via Shubnikov–de Haas (SdH) or de Haas–van Alphen oscillations. The other necessary parameter for finding  $r$  is  $\xi$ , which is found from the measurement of the superconducting critical field versus temperature and the formula  $H_{c2} = \Phi_0/2\pi\mu_0\xi^2$ , or estimated from the size of the superconducting energy gap,  $\Delta$ , and the formula  $\xi = \hbar v_F/2\Delta$ . Note that, for the same Fermi energy, a higher effective mass results in a smaller  $v_F$  and a smaller  $\xi$ , and hence a higher  $H_{orb}^0$ . For this reason, heavy fermion superconductors should favor the FFLO state. In general,  $H_{orb}^0$  comes from critical field measurements and  $H_P$  can be found by analyzing specific heat measurements and determining the superconducting energy gap, as is described in detail below.

## 2. Materials and Methods

Most of the discussion in this article will focus on the crystalline organic conductors. Although the search for inhomogeneous superconductivity has spanned many years, and began in low dimensional single layers of superconducting materials [51], the first credible evidence was from experiments on heavy Fermions such as UPd<sub>2</sub>Al<sub>3</sub>, CeRu<sub>2</sub> [52,53], and CeCoIn<sub>5</sub> [54,55]. These first claims were later found to be incorrect as discussed in Section 3.1. The crystalline organics then became the prime candidates for stabilizing inhomogeneous superconductivity because they are highly anisotropic layered materials, in some cases with incoherent transport between the layers [56–58]. Their high anisotropy allows vortices to hide between the most conducting layers if a magnetic field is aligned precisely parallel to the layers. In this orientation, the vortices have a diminished influence on the superconductivity [59,60]. As explained above, the vortices become Josephson vortices, weak interlayer vortices that can slide in and out of the material in the spaces between the most conducting layers. A vivid illustration of the disappearance of the influence of the vortices is shown in Figure 3. A number of features indicated in the figure such as the critical field,  $H_{c2}$ , the vortex melting transition ( $H_m$ )—the kink below  $H_{c2}$ , the irreversibility transition ( $H_{irr}$ )—the end of the hysteresis, and, at the lowest temperatures flux jumps, can be seen in most of the traces. The last three features, which all depend directly on vortices, are completely absent when the sample layers are parallel (black trace) to the magnetic field. In this orientation, when Josephson vortices are confined to the least conducting layers,  $H_{orb}^0$  is essentially infinite and superconductivity is destroyed by Pauli paramagnetism, resulting in high values of  $\alpha_m$ . Crystalline organic superconductors also can have large mean free paths,  $\ell$ , if they are synthesized carefully. Measurements of  $\ell$  range from 10 to over 100 nm [61]. Given a high value of  $\alpha_m$  and  $r$ , inhomogeneous superconductivity is likely to exist at the right combination of temperature and magnetic field.

A number of different methods have been used to study the FFLO state. A key indication of the existence of the FFLO state is the identification of the phase line separating the traditional vortex superconducting state from the inhomogeneous superconducting state. Given that these are both superconducting states, electrical resistance is always zero and rarely a useful measurement. We have

used rf penetration depth via the tunnel diode oscillator (TDO) method because it is a very sensitive measurement [62] and rather simple and robust, allowing us to use it in dc and pulsed fields [10,63], down to temperatures below 65 mK [64] and in pressure cells [65]. Specific heat is much more difficult to measure, but detailed thermodynamic information is critical to understand the nature of phase transitions [3,55]. NMR is one of the few microscopic probes that have been used to study inhomogeneous superconductivity [7,8,12], and results from an NMR experiment will be discussed in Section 3. Other methods such as magnetic torque [4,5] and thermal conductivity [9] have also been used to locate the phase transitions into and out of the FFLO state.

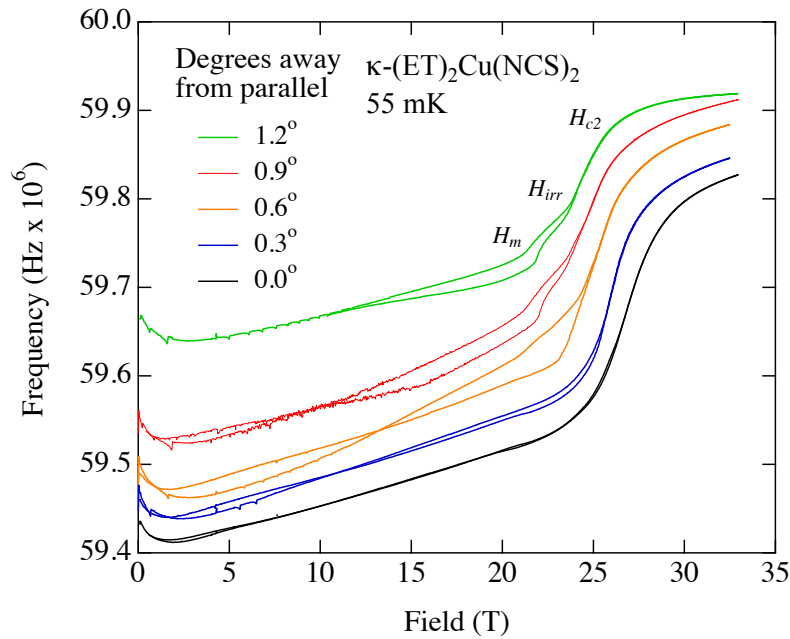


**Figure 3.** The angle dependence of the penetration depth near the parallel orientation for  $\kappa$ ET-CuNCS. The lowest trace is exactly parallel, or  $90^\circ$  in our absolute coordinates. The other traces are in order of increasing angle. The traces are vertically shifted to aid visualization. It is truly remarkable how all the vortex details are absent at the exactly parallel orientation.

### 2.1. The Paramagnetic Limit

A universal property of the FFLO state is that Cooper pairs are broken apart by Pauli paramagnetism as opposed to the formation of vortices. As we described above and as Clogston and Chadrachar [30,31] showed, the ultimate critical magnetic field for a superconductor should occur when the Zeeman energy is greater than the superconducting energy gap. In the simplest case, the Zeeman energy is  $\mu_B H$ , and the BCS energy gap is  $1.746 K_B T_c$ . Of course, most superconductors of current interest are not accurately described by BCS theory, so we use a semi empirical method to find  $H_p$ . As we showed in a previous paper [6], following Clogston [31], we can find the critical magnetic field associated with the quenching of superconductivity by estimating the superconducting energy gap by analyzing specific heat data and setting this energy equal to the gain in free energy in a metal with susceptibility  $\chi_e$ . More specifically, we equate the superconducting condensation energy

$$U_c = 1/2 N(E_f) \Delta(0)^2, \quad (3)$$

where  $N(E_f)$  is the density of states at the Fermi energy and  $\Delta(0)$  is the superconducting energy gap at zero temperature, with

$$\Delta F = 1/2 \mu_0 \chi_e H_p^2, \quad (4)$$

the magnetic energy of a metal with susceptibility  $\chi_e$ . The susceptibility  $\chi_e$  can be expressed as  $\mu_B^2 N(E_f)$ , but it is important to notice that  $\mu_0 H^2$  already has the units of energy density, so  $\chi_e$  must be dimensionless. The expression  $\mu_B^2 N(E_f)$  has dimensions of  $J/T^2 m^3$ , exactly the inverse of  $\mu_0$ . Therefore, we substitute  $\mu_0 \chi_e$  into Equation (4) and after equating  $U_c = \Delta F$  and noticing that the density of states cancels out, we end up with the common result

$$B_P = \frac{\Delta}{\sqrt{2}\mu_B} \quad (5)$$

after using the relation that  $B = \mu_0 H$  and knowing that  $B$  is what we measure in the laboratory. This is the result of a direct comparison of the energy needed to break a Cooper pair with the energy needed to flip a electron spin. Orlando et al. [66] added a correction to Formula (5) of  $1/\sqrt{1+\lambda}$  where  $\lambda$  is the electron–phonon interaction parameter, in order to account for many body effects. This factor was corrected by Schossmann and Carbotte [67] to not have the squareroot in the denominator. McKenzie adds a practical version of this correction to Equation (5) calling it  $g^*/g$  [68], which also takes into account the effects on  $g$ , the gyromagnetic ratio. The result is

$$B_P = \left(\frac{g}{g^*}\right) \frac{\Delta}{\sqrt{2}\mu_B}. \quad (6)$$

The ratio  $g^*/g$  can be found from specific heat and susceptibility measurements, or from spin-splitting of quantum oscillations, a measurement that is common in our laboratory. There is a table with  $g^*/g$  found by both methods in McKenzie’s paper on the arXiv [69]. Despite knowing that  $B_P$  is really the more useful parameter in this calculation, we will continue to use  $H_P$  as the designation of the Chandrasekhar–Clogston Pauli paramagnetic limit as is common in most articles.

## 2.2. Specific Heat, Energy Gap, and Other Parameters

We have found the superconducting energy gap  $\Delta$  by fitting specific heat data in the superconducting state to the Alpha Model, a semi empirical model loosely based on BCS theory, and created by Padamsee et al [70]. Our most recent fits have been done using the more recent version by Johnston [71], which allows direct integration of the specific heat data to find the size of the gap. In this model, the ratio  $\alpha = \Delta/k_B T_c$ , is a free parameter rather than fixing  $\alpha$  at the BCS value of 1.764, although the gap in the model has the same temperature dependence as the BCS model. The calculation is based on the universal expression of the entropy,  $S = k_B \sum f \ln(f)$ , where  $f$  is the Fermi distribution function. The sum can be turned into an integral over the energy range of the quasiparticles, and for a given  $\alpha$ ,  $T_c$ , and  $\gamma$ , the entropy is calculated as a function of temperature. The calculated specific heat can then be found by taking the derivative of the entropy with respect to the temperature. In the Johnston version, the derivative of the entropy integral is done analytically and new integral results that can be used to find the specific heat directly.

We have fit the specific heat of many of the superconductors that we have studied to find the optimal  $\alpha$ , and hence the energy gap  $\Delta$ . One of the additional complications of fitting the specific heat to the Alpha Model is that the fit is sensitive to symmetry of the superconducting order parameter. The original versions of both Padamsee and Johnston use s-wave pairing. We modified the integral expressions for d-wave symmetry. In most cases, we fit the data using both forms of the equation, and pick the best fit to determine  $\alpha$ , and ideally determine the pairing symmetry, a question which is still not completely settled in the organics. We find d-wave as the best fit for  $\kappa$ ET-CuNCS as did Taylor et al. [72], although we find s-wave as the best fit for the other organics, which is contrary to some of the other evidence in, for example, the  $\kappa$ ET-Br material [73]. Part of the challenge in organics is that the lattice is soft, so the phonon contribution to the specific heat continues to low temperatures. One way to subtract the phonon contribution is to measure the specific heat at a magnetic field large enough to quench the superconductivity and subtract that curve from the specific heat measured

with no magnetic field. With this method the phonon contribution is subtracted, but the electronic linear term is also subtracted and mixed with the phonon terms. The linear term determines the constant  $\gamma$ , which is a measure of the electronic density of states. The ability to determine  $\gamma$  is critical to getting a good result for the  $\alpha$  fits. It is unclear what our conclusion should be for the pairing symmetry, particularly if we believe that all the organics have the same pairing. We have also noticed that the shape of the fits are not perfect with s or d-wave pairing, which possibly suggests that the pairing has some other symmetry such as s+d, or anisotropic s-wave, a notion supported by some experiments [74] and recent theory [75]. At this point in time, we will take the best fits, s-wave or d-wave and use that value of  $\alpha$  for each superconductor. Once we have  $\alpha$ , the value of  $H_P$  is then calculated from Equation (6).  $H_P$  is important for the study of the FFLO state because it determines the magnetic field that separates the vortex state of superconductivity from the FFLO state. Given that the superconducting energy gap does not change much in the lower half of the temperature range of the superconducting phase diagram,  $H_P$  and hence the vortex state-FFLO state phase line should be virtually temperature independent [76].

The results of fitting for  $\alpha$  and the corresponding energy gap  $H_P$  are shown for a number of materials in Table 1. We have also collected a number of other useful parameters for the study of inhomogeneous superconductors. Most of the compounds are from the family of organic crystalline superconductors. We have also added the heavy fermion CeCoIn<sub>5</sub> and the pnictides KFe<sub>2</sub>As<sub>2</sub> and LiFeP as examples of other materials where the FFLO state has been claimed to be found.

**Table 1.** Parameters that are useful in the study of inhomogeneous superconductivity. The ratio  $\alpha$  is determined from the specific heat data in the reference next to  $\alpha$ . The other parameters are calculated from values in the table or references. The  $T_c$  values come from the specific heat data referenced for  $\alpha$ .

Material	$\alpha$	$g^*/g$	$T_c$ (K)	$H_P$ (T)	$\alpha_M$	$H_{orb}^0$ (T)	$\xi$ (Å)	$\ell$ (Å)
$\kappa$ -(BEDT-TTF) <sub>2</sub> Cu(NCS) <sub>2</sub>	3.0 [72]	1.26 [69]	9.6	21.6	4.9	130 [35]	13	900 [77]
$\beta''$ -(BEDT-TTF) <sub>2</sub> SF <sub>5</sub> CH <sub>2</sub> CF <sub>2</sub> SO <sub>3</sub>	1.94 [78]	1.0 [69]	4.5	9.2	3.9	75 [35]	21	520
$\alpha$ -(ET) <sub>2</sub> NH <sub>4</sub> Hg(SCN) <sub>4</sub>	1.76 [79]	0.86 [69]	0.96	2.1	5.5	8.1 [76]	53	681 [76]
$\lambda$ -(BETS) <sub>2</sub> GaCl <sub>4</sub>	1.83 [80]	1.0 [69]	4.3	8.3	3.9	23.1 [10]	31.5	170 [56]
$\kappa$ -(ET) <sub>2</sub> Cu[N(CN) <sub>2</sub> ]Br	2.77 [72]	1.4 [69]	11.5	23.8	9.6	161 [81]	12	260 [82]
CeCoIn <sub>5</sub>	3.03 [83,84]	0.73 [83]	2.16	9.44	6.5	43.5 [85]	23	810
KFe <sub>2</sub> As <sub>2</sub>	1.75 [86]	1.3 [87]	3.14	4.84	2.9	9.9	48	1770 [88]
LiFeP	1.89 [89]	1.0	17.6	34.9	2.1	51 [90]	21	5500 [90]

As mentioned earlier, to form an FFLO state,  $H_{orb}^0$  needs to be higher than  $H_P$ , as determined by  $\alpha_M$ . It was determined theoretically that, above the critical value of  $\alpha_M = 1.8$ , the FFLO state could be stabilized [91] in a clean material ( $r > 2$ ). The search for the FFLO state involves careful measurements of some parameter that can be probed in the superconducting state around the value of  $H_P$ , such as specific heat, penetration depth or NMR, in order to find evidence of a phase transition.

### 3. Results and Discussion

The material with the most compelling data that suggests the existence of the FFLO state is  $\kappa$ ET-CuNCS. Evidence for the FFLO state in this material has been found with numerous measurement techniques, including NMR [7,8], rf penetration depth [6,92], magnetic torque [4,5], specific heat [3,93] and transport [5]. The phase diagram of this material depicting examples of these measurements is shown in Figure 4. The phase diagram is certainly suggestive of a FFLO state. Two telling characteristics of the phase line separating the vortex state from the FFLO state are that it occurs at the paramagnetic limit,  $H_P$ , that was calculated with the specific heat data via the Alpha Model, and also that the phase line has near zero slope, consistent with the superconducting energy gap, which is almost temperature independent below  $T_c/2$ .

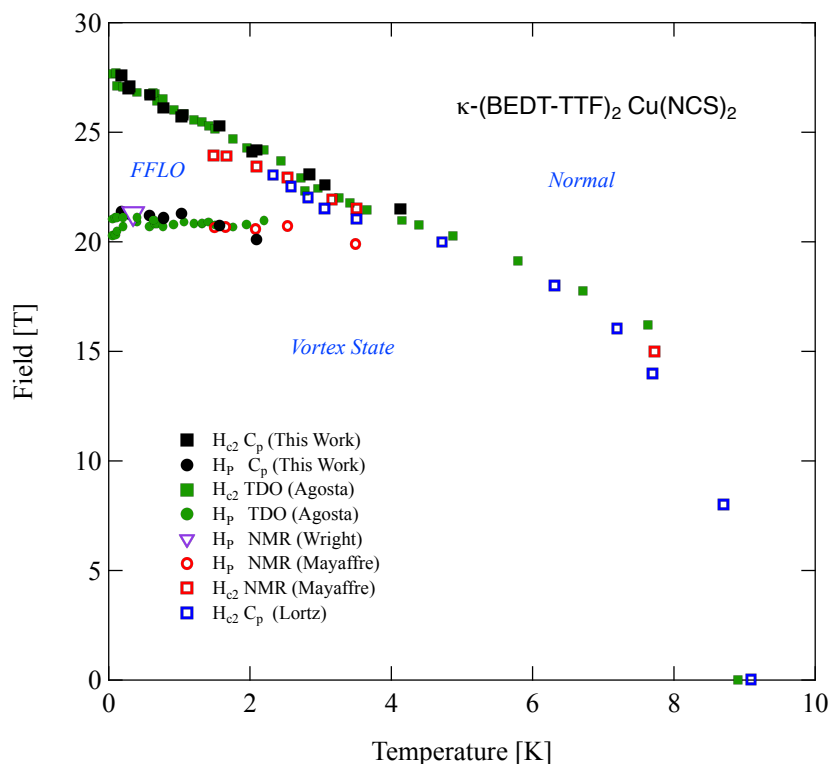


**Figure 4.** Color online. From Agosta et al. [3] Phase diagram of  $\kappa$ ET-CuNCS for parallel magnetic field ( $\theta = 0$ ). Solid black circles represent calorimetric observations of the phase transitions between the lower and higher field superconducting phases at  $H_p$ , and squares, the normal and superconducting state at  $H_{c2}(T)$ . Points from an earlier calorimetric determination of  $H_{c2}(T)$  [93] are shown as open blue squares. Also included are determinations of both the  $H_{c2}$  and  $H_p$  phase boundaries by means of rf penetration measurements (green) [6] and NMR measurements [7,8] (open purple and red symbols, respectively).

Also noteworthy is that the  $H_p$  phase line is a first order transition based on hysteresis in the specific heat as the transition is crossed in up and down sweeps of the magnetic field [3]. An example of the hysteresis in the specific heat is shown in Figure 5a along with a TDO measurement that shows the same hysteresis. The TDO measurement is a much simpler measurement, and the idea that it also can provide evidence of a first order transition is useful for future experiments. The magneto-caloric measurements, shown in Figure 5b, also provided the important evidence that the higher field state has a greater entropy than the vortex state, consistent with the fact that the FFLO state is less ordered than the uniform superconducting state, because of the unpaired electrons [3,94,95]. Another piece of information that can be gathered from the phase diagram is that the enhancement of the ultimate critical field  $H_{c2}$  is  $\approx 1.4H_p$ , consistent with predictions [20,36] for a 2D material. One difference that can be found between this data and the theory is that  $T^*$ , the place where the FFLO phase starts is at  $T_c/3$ , much lower than  $\approx T_c/2$  as most theories predict.

Although this is the best example of the FFLO state, it is worth comparing these results to other materials where credible FFLO states exist. In Figure 6, we show superimposed phase diagrams of three organic conductors where there is evidence for the FFLO state, each normalized by their own experimentally determined  $H_p$  and  $T_c$ . In this figure, the three materials scale relatively well, although the upper critical field for  $\lambda$ BETS-GaCl is not quite as high as the others. This would suggest that it is not as two-dimensional as the other superconductors [20], however, we have used the vortex-FFLO phase line as the  $H_p$  for this figure. It is also possible that impurities or spin-orbit scattering could have raised the value of  $H_p$  [32,48].

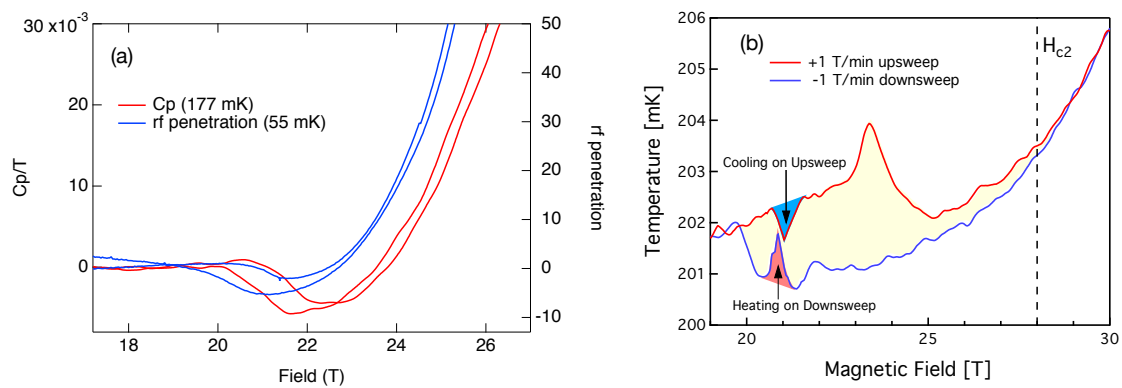


**Figure 5.** Color online. (a) specific heat and TDO up and down field traces as the measurements cross the vortex-FFLO phase transition showing the hysteresis. This is direct evidence of a first order transition; (b) from Agosta et al. [3], the magneto caloric effect, which shows the direction of the flow of latent heat as the vortex-FFLO phase line is crossed. This information can be used to show that the higher field state, in this case the FFLO state, is of higher entropy than the vortex state, consistent with what is expected for this phase transition [3,94,95].

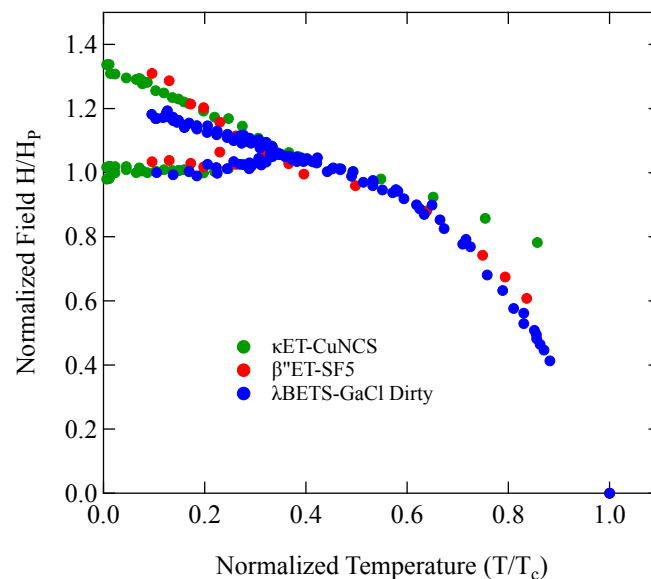


**Figure 6.** Color online. Phase diagram of  $\kappa$ ET-CuNCS,  $\lambda$ BETS-GaCl and  $\beta''$ ET-SF5 each normalized using the phase line between the vortex and FFLO states. The BETS does not seem to have as much enhancement of the upper critical field as the other two superconductors, which scale identically.

To probe these ideas, we have preliminary data for cleaner samples of BETS, synthesized by Kobayashi, and the data suggest that the scattering details may be important. In Figure 7, we show preliminary new data on an absolute scale with the previous data. The cleaner samples have a lower  $H_p$ , but surprisingly an identical  $H_{c2}$ . The drop in the value of  $H_p$  is expected if it is dependent on similar pair breaking mechanisms as  $H_{c2}$  [32,48]. In particular, less spin-orbit scattering should lower the critical field. The surprise is that the upper critical field for the FFLO state, where the material crosses into the normal state, is robust with respect to the degree of scattering, unlike  $H_p$ , the upper critical field for the vortex state. In the traditional superconducting state,  $H_{c2}$  is very sensitive to scattering. This may be understandable in the context of  $H_{c2}$  as calculated by [32,48] where similar changes in the  $H_{c2}$  phase line are found for greater orbital effects (vortices) or more spin orbit scattering. However, spin-orbit scattering can directly modify  $H_p$ , but vortex effects will not. In addition, if orbital (vortex) effects are suppressed, as they are in the highly anisotropic organics,  $H_{c2}$  must be the result

of the magnetic energy in the system, which is more immune to scattering events than orbital effects. Therefore, the vortex FFLO phase line should follow  $H_P$ , which is dependent on the energy gap and spin orbit scattering, and  $H_{c2}$  will be insensitive to scattering. In many of these materials, it may be important to always adjust  $H_P$  to account for the degree of scattering and spin-orbit scattering to properly interpret the results.

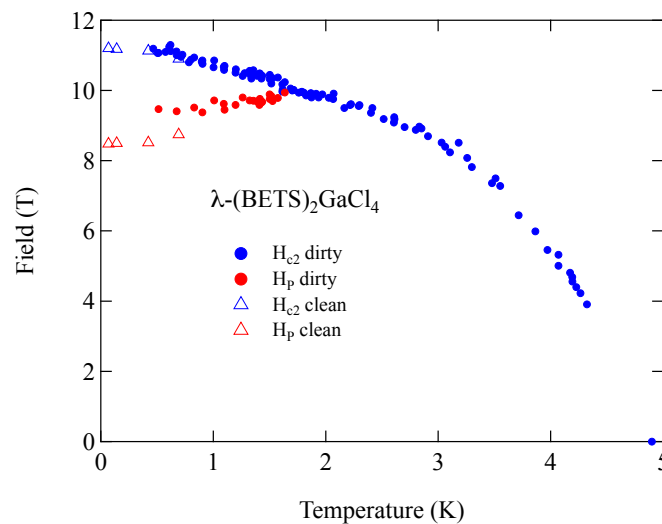


**Figure 7.** We obtained new samples from Kobayashi that are higher quality samples (more pure) based on Shubnikov–de Haas oscillations. The higher quality samples show on an absolute scale that the upper critical field of the clean and dirty samples is the same, but  $H_P$  is very sensitive to impurities. The new data was taken in a dilution refrigerator and we are looking forward to extending the data to higher temperatures in the near future.

One of the more promising measurements showing further evidence for the FFLO state was made with NMR by Koutroulakis et al. [12] on the crystalline organic  $\beta''$ ET-SF5. In this measurement, the line shape of carbon atoms in the FFLO phase was measured and compared to a calculated line shape. The signal comes from the substitution of four inequivalent carbon atoms in the ET molecule with  $^{13}\text{C}$  to have an active NMR target. The data is compared to a calculation based on the sum of the four inequivalent line-shapes from the four inequivalent carbon atoms modified by the effects of a one-dimensional  $\mathbf{q}$ -vector. It is not yet clear if the features of the line-shape are unique enough to offer proof that the FFLO state is the cause of the line-shape, but it is more compelling than any other microscopic measurement so far. The data is reproduced in Figure 8.

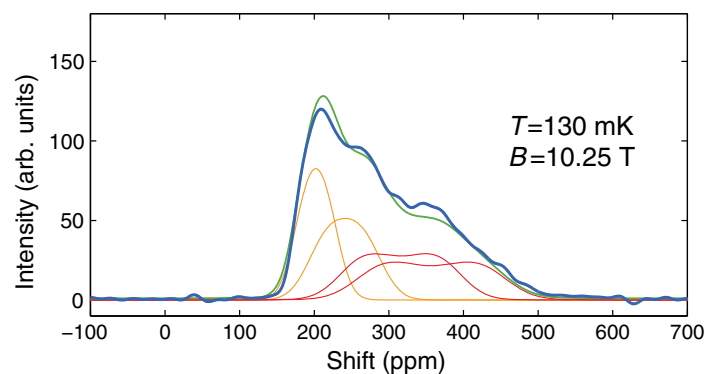


**Figure 8.** Color online. Example of spectrum simulation compared to recorded spectrum (blue) from Koutroulakis et al. [12]. The simulation is a sum (green) of four Gaussian-broadened contributions (red, orange) arising from a single-Q sinusoidal modulation of the SC order parameter.

### 3.1. Other Materials

Two other materials outside of the class of organic conductors are worth mentioning: the heavy Fermion superconductor CeCoIn<sub>5</sub> and the pnictide superconductor KFe<sub>2</sub>As<sub>2</sub>. An interesting discussion of the FFLO state in heavy fermion and pnictide superconductors was recently published that supports the existence of inhomogeneous superconductivity in these classes of materials [37]. The heavy fermion superconductor CeCoIn<sub>5</sub> was one of the first materials where there was thought to be credible experimental evidence for the FFLO state. This evidence was in the form of calorimetric observations of a bulk field induced phase transition between two superconducting phases [54,55]. This transition was initially attributed to FFLO superconductivity but is now known to correspond to the onset of spin-density wave (SDW) ordering within the superconducting state [95–99] and is called the Q state. The Q state is the coexistence of a SDW and a superconducting state, although it is not clear if the superconducting state is a FFLO state or a uniform state. The  $\mathbf{q}$ -vector measured by neutron scattering suggests a modulated state, but it does not change wavelength as a function of magnetic field as is expected for the FFLO state [97]. Details of the SDW ordering observed by NMR have led to suggestions of a lower field FFLO transition [100] and/or coupling of a FFLO phase to this SDW transition [100–102], but there is no clear thermodynamic evidence for these proposals [95,103,104]. The possibility remains of a more complex coupling of the SDW transition to a modified FFLO phase or pair density wave (PDW) [100,104]. One way to gain more insight into the nature of the Q phase is to scale the CeCoIn<sub>5</sub> data on the same phase diagram with an organic superconductor as seen in Figure 9. In this figure, the TDO data from ETCuNCS is used as a baseline, and the CeCoIn<sub>5</sub> data is scaled using  $H_p$  from Table 1. We note that  $\alpha$  for CeCoIn<sub>5</sub> was calculated based on two sets of specific heat data [83,84] with nearly identical results. The parameter  $g^*/g$  was more difficult to determine, and for this study we relied on  $\gamma$  and  $\chi$  measurements [83] averaged over temperatures below  $T_c$  and used Wilson's ratio [69]. What is surprising is that although the vortex-FFLO phase line found by specific heat and torque does not line up with  $H_p$ , and it also wouldn't even have the right slope for the  $H_p$  line, the phase line found by TDO rf penetration measurements [64] matches the value of  $H_p$  as calculated from the specific heat. Adding to this evidence for a phase line at 9.2 T, Koutroulakis et al. [100] identified a phase they call the exotic superconducting state, or ESC that starts at a minimum magnetic field of 9.2 T. It may be worth looking at the CeCoIn<sub>5</sub> specific heat data to see if there is any indication of this lower phase line. In any case, it can be seen that the Q state, as it is called, is not a simple FFLO state, or at least not the same as found in the organic and pnictide superconductors.

The pnictides are not nearly as anisotropic as the organics [90], but their high electron masses and tunable anisotropy suggest that they may be candidates for inhomogeneous superconductivity [105,106]. A very recent result claims the possible existence of a FFLO state in the two band pnictide superconductor KFe<sub>2</sub>As<sub>2</sub> [107] based on specific heat and magnetic torque measurements. Using the values of  $\alpha$  from the two band alpha model in this KFe<sub>2</sub>As<sub>2</sub> paper and others [86,108], we calculated  $H_p$  between 4.45 and 5.23 T (the result in Table 1 is the average). For convenience, we used the value from Figure 4 in Cho et al. [107] to scale their phase diagram and superimpose it on the the phase diagram from the organic conductors. The result is in Figure 10. This diagram and the KFe<sub>2</sub>As<sub>2</sub> specific heat data raise a number of questions about the claim of the FFLO state in this material.

The enhancement of the critical field over  $H_p$  in  $\kappa$ ET-CuNCS is 1.35, and in KFe<sub>2</sub>As<sub>2</sub> it is 1.24 if you extrapolate to zero temperature. This is consistent with the difference in anisotropy. According to Matsuda [20], the enhancement in an ideal 2D and 3D system should be 1.4 and 1.2 respectively. The ratio of parallel and perpendicular critical fields at zero temperature is one indication of the anisotropy of a material, and this value is ~4–5 for both KFe<sub>2</sub>As<sub>2</sub> [86] and for  $\kappa$ ET-CuNCS, yet this is misleading because  $\kappa$ ET-CuNCS is strongly paramagnetically limited. Using the initial slopes of the critical field lines in different orientations as described in Section 1.2, Equation (2) determines  $H_{orb}^0$ .  $H_{orb}^0$  is a much better measure of the superconducting anisotropy because it is based on the anisotropy of the vortices, and hence the superconducting coherence lengths,  $\xi$ . This anisotropy measurement is reliable as long

as the diameter of the vortices is larger than the interlayer spacing, a limit that is always true close to  $T_c$  where  $\xi$  diverges. Using these slopes, the anisotropy of  $\text{KFe}_2\text{As}_2$  is still 4.5 but for  $\kappa\text{ET-CuNCS}$  the anisotropy is  $\approx 21$ , if the slope of  $H_{c2}$  is properly measured [93]. Thus, this anisotropy explains the difference in critical field enhancement, but the anisotropy of  $\text{KFe}_2\text{As}_2$  is inconsistent with the onset of the FFLO state in a multiband superconductor. According to Gurevich [42], the lower anisotropy of the pnictides should result in the FFLO state starting at  $t < 0.5$ , below the results found by Cho et al., and certainly below the results of the highly anisotropic organic conductors. Zocco et al. [88] has a higher temperature onset of the FFLO state according to their calculations, but a much smaller critical field enhancement than the data.

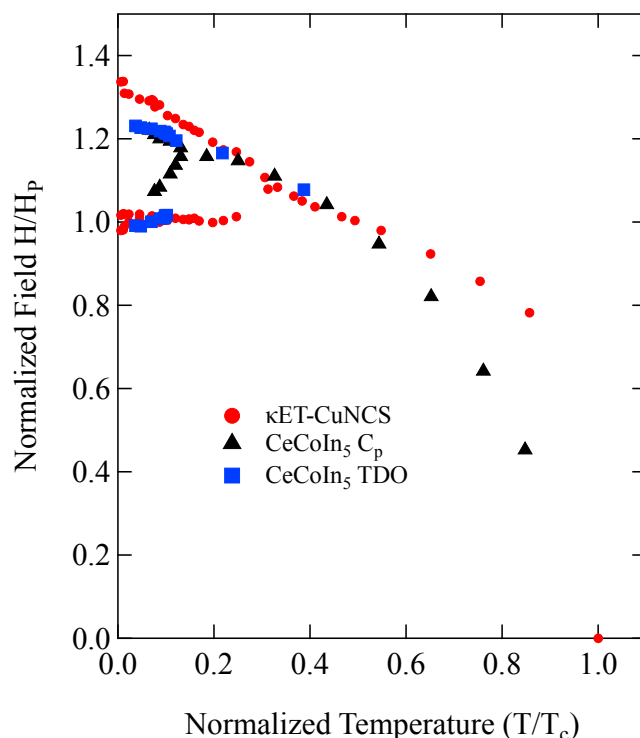


**Figure 9.** Color online. Phase diagram of  $\text{CeCoIn}_5$  with  $\kappa\text{ET-CuNCS}$  as our baseline FFLO phase diagram. If the magnetic field is normalized by  $H_p$  as calculated by Equation (6), the TDO measurement [64] (blue squares) finds a phase line at  $H_p$ . NMR experiments [100] confirm a change of the material properties at this field value too, suggesting that there may be a FFLO type transition at the calculated  $H_p$ . The more vertical phase line discovered by specific heat [54] (black triangles) at about  $t = 0.1$  could be related to the SDW.

The second quantitative difference between the organic phase diagrams and the  $\text{KFe}_2\text{As}_2$  phase diagram is the slope of the vortex state–FFLO state phase line at  $H_p$ . As expected, to first order, this line should have no slope if  $H_p$  is proportional to the energy gap, given that the BCS superconducting energy gap is almost constant for  $t < 0.4$ . Within experimental error, this is almost the case for  $\kappa\text{ET-CuNCS}$ . Doing a fit to our largest set of data points, from the TDO measurements, we find a slope of  $< 0.05$  T/K. The slope of this phase line for  $\text{KFe}_2\text{As}_2$  is 0.3 T/K. The increased slope could be due to the presence of vortices, as expected for the pnictides, which are less anisotropic than the organic superconductors. Another interpretation is that this line is really  $H_{c2}$  and the bump in specific heat at a higher field is not due to the FFLO state. Given the form of the specific heat data in Agosta et al. [3] and the calculations of Ptok [106], a small jump in specific heat at  $H_{c2}$  followed by a large jump in specific heat at the FFLO to uniform superconductivity phase line does not make sense. In Ptok, these jumps are calculated as at least similar in size, and given that  $H_{c2}$  is a transition into a bulk

superconducting state, with the formation of Cooper pairs throughout the sample, the resulting drop in entropy should produce a robust specific heat peak at  $H_{c2}$ , and as calculated in Ptok and in many publications for single band superconductors [109]. Furthermore, without more angular data to see if the specific heat signature of the FFLO state slowly changes when the sample is rotated with respect to the magnetic field, the data is less compelling. Many of the other studies of  $\text{KFe}_2\text{As}_2$  that have been done, as referenced in the above paragraph, and in particular the one by Zocco et al., do not see any indication of a FFLO state. There still is hope to find indications of the FFLO state in  $\text{KFe}_2\text{As}_2$  and other pnictides, but the present claim in Cho et al. although exciting, needs more evidence.

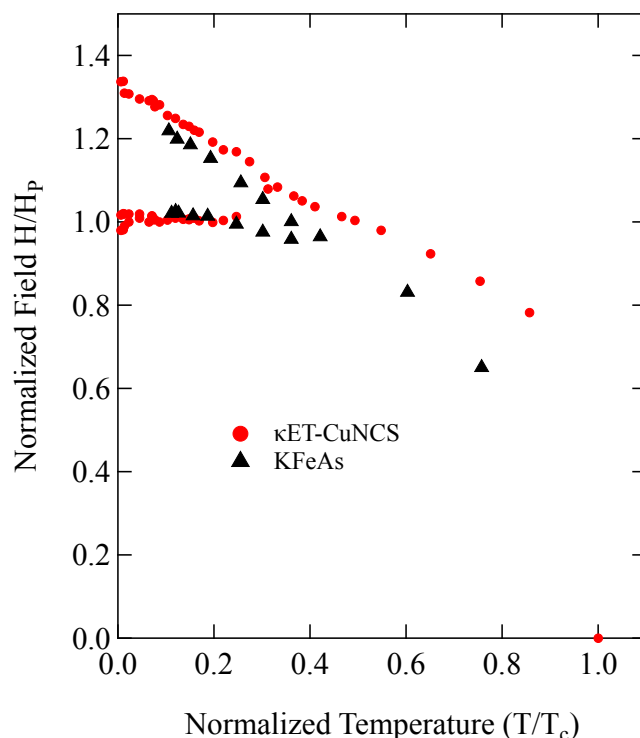


**Figure 10.** Color online. The phase diagram of  $\kappa\text{ET-CuNCS}$  superimposed with the  $\text{KFe}_2\text{As}_2$  data from Cho et al. [107], normalized to  $T_c$  and  $H_p$  for each sample respectively. We note the two main differences, the slope of the vortex-FFLO transition, and the overall enhancement of the FFLO state over  $H_p$ .

### 3.2. New Materials

There have been predictions of the FFLO state in  $\text{LiFeP}$  [90], and this is another good example of a material where it is difficult to predict if the FFLO state exists.  $\text{LiFeP}$  as many of the pnictides, has two superconducting energy gaps, and it is unclear, when there are multiple gaps, which one dominates. It is reasonable to think that the largest gap, with the largest  $T_c$  will dominate. This is because above  $H_p$  for the largest gap, all Cooper pairs will be subject to pair breaking via the Zeeman energy. The data claiming inhomogeneous superconductivity in  $\text{KFe}_2\text{As}_2$  [107], if it is correct, shows the  $H_p$  phase line at the value of the higher gap energy consistent with the argument above. For this reason, the parameters for both of the pnictides in Table 1 correspond to the higher energy of the two gaps found in each compound. The energy gaps and ratio  $\alpha$  for these materials were not calculated from our version of the alpha model but came from the papers referenced in the table, and use a two gap model. It is also important to note that  $g^*/g$  for  $\text{LiFeP}$  is not known, so it was set equal one. Given what is known, the value of  $H_p$  in  $\text{LiFeP}$  is above  $H_{c2}$  and no FFLO state should exist. It is possible that a weak variation of the FFLO state could exist when the magnetic field was greater than

$H_P$  corresponding to the lower energy gap, but it is difficult to search for evidence of such a weak FFLO state, if it exists at all.

#### 4. Conclusions

It is clear that an exotic superconducting state exists in the low temperature high field quadrant of the superconducting phase diagram in quasi 2D anisotropic organic superconductors, and possibly heavy fermion and pnictide superconductors. So far, the data that have been collected on the organics is consistent with inhomogeneous superconductivity. Microscopic probes such as NMR will help determine if these are truly FFLO states, but spatial probes such as STM, neutrons, or X-rays will eventually be the way to measure the  $\mathbf{q}$ -vectors, and unambiguously identify these exotic correlated electron states. There are still many methods available for the organics that can be used to expand the parameter phase space, including pressure, defects, and chemical substitution. It has been shown that CeCoIn<sub>5</sub> is more complex than the other materials, and the specific heat data needs a second look. It also may be a good candidate for STM. Other classes of superconductors such as the pnictides are promising new materials for understanding inhomogeneous superconductivity. Finally, a topic not covered in this review, and closely related theoretically [110,111] and experimentally [112] to this subject is the study of inhomogeneous superconductivity in quasi 1D materials. It will be insightful to discuss 1D and 2D materials together in the future.

**Acknowledgments:** The author thanks Andrei Lebed for helpful discussions. A portion of this work was performed at the National High Magnetic Field Laboratory, which is supported by National Science Foundation Cooperative Agreement No. DMR-11157490 and the state of Florida.

**Conflicts of Interest:** The author declares no conflict of interest.

#### References

1. Fulde, P.; Ferrell, R.A. Superconductivity in a Strong Spin-Exchange Field. *Phys. Rev.* **1964**, *135*, A550–A563, doi:10.1103/PhysRev.135.A550.
2. Larkin, A.I.; Ovchinnikov, Y.N. Inhomogeneous State of Superconductors. *Sov. Phys. JETP* **1965**, *20*, 762–769.
3. Agosta, C.C.; Fortune, N.A.; Hannahs, S.T.; Gu, S.; Liang, L.; Park, J.H.; Schlueter, J.A. Calorimetric Measurements of Magnetic-Field-Induced Inhomogeneous Superconductivity Above the Paramagnetic Limit. *Phys. Rev. Lett.* **2017**, *118*, 267001, doi:10.1103/PhysRevLett.118.267001.
4. Bergk, B.; Demuer, A.; Sheikin, I.; Wang, Y.; Wosnitzer, J.; Nakazawa, Y.; Lortz, R. Magnetic torque evidence for the Fulde-Ferrell-Larkin-Ovchinnikov state in the layered organic superconductor  $\kappa$ -(BEDT-TTF)<sub>2</sub>Cu(NCS)<sub>2</sub>. *Phys. Rev. B* **2011**, *83*, 064506.
5. Tsuchiya, S.; Yamada, J.i.; Sugii, K.; Graf, D.; Brooks, J.S.; Terashima, T.; Uji, S. Phase Boundary in a Superconducting State of  $\kappa$ -(BEDT-TTF)<sub>2</sub>Cu(NCS)<sub>2</sub>: Evidence of the Fulde-Ferrell-Larkin-Ovchinnikov Phase. *J. Phys. Soc. Jpn.* **2015**, *84*, 034703, doi:10.7566/JPSJ.84.034703.
6. Agosta, C.C.; Jin, J.; Coniglio, W.A.; Smith, B.E.; Cho, K.; Stroe, I.; Martin, C.; Tozer, S.W.; Murphy, T.P.; Palm, E.C.; et al. Experimental and semiempirical method to determine the Pauli-limiting field in quasi-two-dimensional superconductors as applied to  $\kappa$ -(BEDT-TTF)<sub>2</sub>Cu(NCS)<sub>2</sub>: Strong evidence of a FFLO state. *Phys. Rev. B* **2012**, *85*, 214514.
7. Wright, J.A.; Green, E.; Kuhns, P.; Reyes, A.; Brooks, J.; Schlueter, J.; Kato, R.; Yamamoto, H.; Kobayashi, M.; Brown, S.E. Zeeman-Driven Phase Transition within the Superconducting State of  $\kappa$ -(BEDT-TTF)<sub>2</sub>Cu(NCS)<sub>2</sub>. *Phys. Rev. Lett.* **2011**, *107*, 087002, doi:10.1103/PhysRevLett.107.087002.
8. Mayaffre, H.; Kramer, S.; Horvatić, M.; Berthier, C.; Miyagawa, K.; Kanoda, K.; Mitrović, V.F. Evidence of Andreev bound states as a hallmark of the FFLO phase in  $\kappa$ -(BEDT-TTF)<sub>2</sub>Cu(NCS)<sub>2</sub>. *Nat. Phys.* **2014**, *10*, 928–932, doi:10.1038/nphys3121.
9. Tanatar, M.A.; Ishiguro, T.; Tanaka, H.; Kobayashi, H. Magnetic field-temperature phase diagram of the quasi-two-dimensional organic superconductor  $\lambda$ -(BETS)<sub>2</sub>GaCl<sub>4</sub> studied via thermal conductivity. *Phys. Rev. B* **2002**, *66*, 134503.

10. Coniglio, W.A.; Winter, L.E.; Cho, K.; Agosta, C.C.; Fravel, B.; Montgomery, L.K. Superconducting phase diagram and FFLO signature in  $\lambda$ -(BETS)<sub>2</sub>GaCl<sub>4</sub> from rf penetration depth measurements. *Phys. Rev. B* **2011**, *83*, 224507, doi:10.1103/PhysRevB.83.224507.
11. Cho, K.; Smith, B.E.; Coniglio, W.A.; Winter, L.E.; Agosta, C.C.; Schlueter, J.A. Upper critical field in the organic superconductor  $\beta''$ -(ET)<sub>2</sub>SF<sub>5</sub>CH<sub>2</sub>CF<sub>2</sub>SO<sub>3</sub>: Possibility of Fulde-Ferrell-Larkin-Ovchinnikov state. *Phys. Rev. B* **2009**, *79*, 220507, doi:10.1103/PhysRevB.79.220507.
12. Koutroulakis, G.; Kuhne, H.; Schlueter, J.A.; Wosnitza, J.; Brown, S.E. Microscopic Study of the Fulde-Ferrell-Larkin-Ovchinnikov State in an All-Organic Superconductor. *Phys. Rev. Lett.* **2016**, *116*, 067003, doi:10.1103/PhysRevLett.116.067003.
13. Burkhardt, H.; Rainer, D. Fulde-Ferrell-Larkin-Ovchinnikov state in layered superconductors. *Ann. Phys.* **1994**, *506*, 181–194.
14. Buzdin, A.I.; Kachkachi, H. Generalized Ginzburg-Landau theory for nonuniform FFLO superconductors. *Phys. Lett. A* **1997**, *225*, 341–348, doi:10.1016/S0375-9601(96)00894-8.
15. Houzet, M.; Buzdin, A. Influence of the paramagnetic effect on the vortex lattice in 2D superconductors. *EPL (Europhys. Lett.)* **2000**, *50*, 375.
16. Klein, U.; Rainer, D.; Shimahara, H. Interplay of Fulde-Ferrell-Larkin-Ovchinnikov and Vortex States in Two-Dimensional Superconductors. *J. Low Temp. Phys.* **2000**, *118*, 91–104.
17. Shimahara, H. Fulde-Ferrell state in quasi-two-dimensional superconductors. *Phys. Rev. B* **1994**, *50*, 12760, doi:10.1103/PhysRevB.50.12760.
18. Agterberg, D.F.; Yang, K. The effect of impurities on Fulde-Ferrell-Larkin-Ovchinnikov superconductors. *J. Phys. Cond. Matt.* **2001**, *13*, 9259–9270, doi:10.1088/0953-8984/13/41/315.
19. Houzet, M.; Meurdesoif, Y.; Coste, O.; Buzdin, A. Structure of the non-uniform Fulde-Ferrell-Larkin-Ovchinnikov state in 3D superconductors. *Phys. C Superconduct.* **1999**, *316*, 89–96.
20. Matsuda, Y.; Shimahara, H. Fulde-Ferrell-Larkin-Ovchinnikov State in Heavy Fermion Superconductors. *J. Phys. Soc. Jpn.* **2007**, *76*, 051005.
21. Piazza, F.; Zwerger, W.; Strack, P. FFLO strange metal and quantum criticality in two dimensions: Theory and application to organic superconductors. *Phys. Rev. B* **2016**, *93*, 085112, doi:10.1103/PhysRevB.93.085112.
22. Kinnunen, J.J.; Baarsma, J.E.; Martikainen, J.P.; Törmä, P. The Fulde-Ferrell-Larkin-Ovchinnikov state for ultracold fermions in lattice and harmonic potentials: A review. *Rep. Prog. Phys.* **2018**, *81*, 046401, doi:10.1088/1361-6633/aaa4ad.
23. Zwierlein, M.W.; Schirotzek, A.; Schunck, C.H.; Ketterle, W. Fermionic Superfluidity with Imbalanced Spin Populations. *Science* **2006**, *311*, 492–496, doi:10.1126/science.1122318.
24. Liao, Y.A.; Rittner, A.S.C.; Paprotta, T.; Li, W.; Partridge, G.B.; Hulet, R.G.; Baur, S.K.; Mueller, E.J. Spin-imbalance in a one-dimensional Fermi gas. *Nature* **2010**, *467*, 567–569.
25. Heidrich-Meisner, F.; Orso, G.; Feiguin, A.E. Phase separation of trapped spin-imbanced Fermi gases in one-dimensional optical lattices. *Phys. Rev. A* **2010**, *81*, 1136–1137, doi:10.1103/PhysRevA.81.053602.
26. Olsen, B.A.; Revelle, M.C.; Fry, J.A.; Sheehy, D.E.; Hulet, R.G. Phase diagram of a strongly interacting spin-imbanced Fermi gas. *Phys. Rev. A* **2015**, *92*, 063616, doi:10.1103/PhysRevA.92.063616.
27. Korolyuk, A.; Massel, F.; Törmä, P. Probing the Fulde-Ferrell-Larkin-Ovchinnikov Phase by Double Occupancy Modulation Spectroscopy. *Phys. Rev. Lett.* **2010**, *104*, 236402, doi:10.1103/PhysRevLett.104.236402.
28. Paglione, J.; Greene, R.L. High-temperature superconductivity in iron-based materials. *Nat. Phys.* **2010**, *6*, 645–658, doi:10.1038/nphys1759.
29. Stewart, G.R. Unconventional superconductivity. *Adv. Phys.* **2017**, *66*, 75–196, doi:10.1080/00018732.2017.1331615.
30. Chandrasekhar, B.S. A Note on the Maximum Critical Field of High-Field Superconductors. *Appl. Phys. Lett.* **1962**, *1*, 7, doi:10.1063/1.1777362.
31. Clogston, A.M. Upper Limit for the Critical Field in Hard Superconductors. *Phys. Rev. Lett.* **1962**, *9*, 266–267, doi:10.1103/PhysRevLett.9.266.
32. Klemm, R.A.; Luther, A.; Beasley, M.R. Theory of the upper critical field in layered superconductors. *Phys. Rev. B* **1975**, *12*, 877–891, doi:10.1103/PhysRevB.12.877.
33. Saint-James, D.; Sarma, G.; Thomas, E.J. *Type II Superconductivity*; Saint-James, D., Sarma, G., Thomas, E.J., Eds.; International Series of Monographs on Natural Philosophy; Pergamon Press: Oxford, NY, USA, 1969; Volume 17.

34. Casalbuoni, R.; Nardulli, G. Inhomogeneous superconductivity in condensed matter and QCD. *Rev. Mod. Phys.* **2004**, *76*, 263–320, doi:10.1103/RevModPhys.76.263.
35. Wosnitza, J. FFLO States in Layered Organic Superconductors. *Annalen der Physik* **2018**, *530*, 1700282, doi:10.1002/andp.201700282.
36. Zwicknagl, G.; Wosnitza, J. Breaking Translational Invariance By Population Imbalance: The Fulde-Ferrell-Larkin-Ovchinnikov States. *Int. J. Mod. Phys. B* **2010**, *24*, 3915–3949, doi:10.1142/S0217979210056396.
37. Ptok, A.; Kapcia, K.J.; Piekarz, P.; Oleś, A.M. The ab initio study of unconventional superconductivity in CeCoIn<sub>5</sub> and FeSe. *New J. Phys.* **2017**, *19*, 063039, doi:10.1088/1367-2630/aa6d9d.
38. Denisov, D.; Buzdin, A.; Shimahara, H. Types of Fulde-Ferrell-Larkin-Ovchinnikov states induced by anisotropy effects. *Phys. Rev. B* **2009**, *79*, 064506.
39. Croitoru, M.D.; Buzdin, A.I. Resonance in-plane magnetic field effect as a means to reveal the Fulde-Ferrell-Larkin-Ovchinnikov state in layered superconductors. *Phys. Rev. B* **2012**, *86*, 064507, doi:10.1103/PhysRevB.86.064507.
40. Ptok, A. The influence of the dimensionality of the system on the realization of unconventional Fulde-Ferrell-Larkin-Ovchinnikov pairing in ultra-cold Fermi gases. *J. Phys. Condens. Matter* **2017**, *29*, 475901, doi:10.1088/1361-648X/aa928d.
41. Croitoru, M.D.; Houzet, M.; Buzdin, A.I. In-Plane Magnetic Field Anisotropy of the Fulde-Ferrell-Larkin-Ovchinnikov State in Layered Superconductors. *Phys. Rev. Lett.* **2012**, *108*, 207005.
42. Gurevich, A. Upper critical field and the Fulde-Ferrell-Larkin-Ovchinnikov transition in multiband superconductors. *Phys. Rev. B* **2010**, *82*, 184504, doi:10.1103/PhysRevB.82.184504.
43. Bulaevskii, L.N. Inhomogeneous state and the anisotropy of the upper critical field in layered superconductors with Josephson layer interaction. *Zhurnal Eksperimentalnoi i Teoreticheskoi Fiziki* **1974**, *38*, 1278–1288.
44. Mola, M.M.; King, J.T.; McRaven, C.P.; Hill, S.; Qualls, J.S.; Brooks, J.S. Josephson plasma resonance in  $\kappa$ -(BEDT-TTF)<sub>2</sub>Cu(NCS)<sub>2</sub>. *Phys. Rev. B* **2000**, *62*, 5965–5970, doi:10.1103/PhysRevB.62.5965.
45. Hill, S.; Mola, M.M.; Qualls, J.S. Interlayer electrodynamics in the organic superconductor  $\kappa$ -(BEDT-TTF)<sub>2</sub>Cu(NCS)<sub>2</sub> (BEDT-TTF = bis-ethylenedithio-tetrathiafulvalene): Evidence for a transformation within the vortex state. *J. Phys. Condens. Matter* **2002**, *14*, 6701.
46. Kirtley, J.R.; Moler, K.A.; Schlueter, J.A.; Williams, J.M. Inhomogeneous interlayer Josephson coupling in  $\kappa$ -(BEDT-TTF)<sub>2</sub>Cu(NCS)<sub>2</sub>. *J. Phys. Condens. Matter* **1999**, *11*, 2007–2016.
47. Lebed, A.G. Orbital effect for the Fulde-Ferrell-Larkin-Ovchinnikov phase in a quasi-two-dimensional superconductor in a parallel magnetic field. *Phys. Rev. B* **2018**, *97*, 144504, doi:10.1103/PhysRevB.97.144504.
48. Werthamer, N.R.; Helfand, E.; Hohenberg, P.C. Temperature and Purity Dependence of the Superconducting Critical Field,  $H_{c2}$ . III. Electron Spin and Spin-Orbit Effects. *Phys. Rev.* **1966**, *147*, 295–302, doi:10.1103/PhysRev.147.295.
49. Schneider, T.; Schmidt, A. Dimensional crossover in the upper critical field of layered superconductors. *Phys. Rev. B* **1993**, *47*, 5915–5921, doi:10.1103/PhysRevB.47.5915.
50. Ptok, A. The Fulde-Ferrell-Larkin-Ovchinnikov Superconductivity in Disordered Systems. *Acta Phys. Pol. A* **2010**, *118*, 420–422, doi:10.12693/aphyspola.118.420.
51. Tedrow, P.M.; Meservey, R. Spin-Paramagnetic Effects in Superconducting Aluminum Films. *Phys. Rev. B* **1973**, *8*, 5098–5108, doi:10.1103/PhysRevB.8.5098.
52. Gloos, K.; Modler, R.; Schimanski, H.; Bredl, C.D.; Geibel, C.; Steglich, F.; Buzdin, A.I.; Sato, N.; Komatsubara, T. Possible formation of a nonuniform superconducting state in the heavy-fermion compound UPd<sub>2</sub>Al<sub>3</sub>. *Phys. Rev. Lett.* **1993**, *70*, 501–504, doi:10.1103/PhysRevLett.70.501.
53. Tachiki, M.; Takahashi, S.; Gegenwart, P.; Weiden, M.; Lang, M.; Geibel, C.; Steglich, F.; Modler, R.; Paulsen, C.; Ōnuki, Y. Generalized Fulde-Ferrell-Larkin-Ovchinnikov state in heavy-fermion and intermediate-valence systems. *Z. Phys. B Condens. Matter* **1997**, *100*, 369–380, doi:10.1007/s002570050135.
54. Radovan, H.A.; Fortune, N.A.; Murphy, T.P.; Hannahs, S.T.; Palm, E.C.; Tozer, S.W.; Hall, D. Magnetic enhancement of superconductivity from electron spin domains. *Nature* **2003**, *425*, 51–55. doi:10.1038/nature01842.
55. Bianchi, A.; Movshovich, R.; Capan, C.; Pagliuso, P.G.; Sarrao, J.L. Possible Fulde-Ferrell-Larkin-Ovchinnikov Superconducting State in CeCoIn<sub>5</sub>. *Phys. Rev. Lett.* **2003**, *91*, 187004, doi:10.1103/physrevlett.91.187004.

56. Mielke, C.; Singleton, J.; Nam, M.S.; Harrison, N.; Agosta, C.C.; Fravel, B.; Montgomery, L.K. Superconducting properties and Fermi-surface topology of the quasi-two-dimensional organic superconductor  $\lambda$ -(BETS)<sub>2</sub>GaCl<sub>4</sub> (BETS=; bis(ethylene-dithio)tetraselenafulvalene). *J. Phys. Condens. Matter* **2001**, *13*, 8325–8345.
57. Singleton, J.; Goddard, P.; Ardavan, A.; Harrison, N.; Blundell, S.; Schlueter, J.; Kini, A. Test for interlayer coherence in a quasi-two-dimensional superconductor. *Phys. Rev. Lett.* **2002**, *88*, 037001.
58. Singleton, J.; Goddard, P.A.; Ardavan, A.; Coldea, A.I.; Blundell, S.J.; McDonald, R.D.; Tozer, S.; Schlueter, J.A. Persistence to High Temperatures of Interlayer Coherence in an Organic Superconductor. *Phys. Rev. Lett.* **2007**, *99*, 027004, doi:10.1103/PhysRevLett.99.027004.
59. Mansky, P.A.; Chaikin, P.M.; Haddon, R.C. Vortex lock-in state in a layered superconductor. *Phys. Rev. Lett.* **1993**, *70*, 1323–1326, doi:10.1103/PhysRevLett.70.1323.
60. Mansky, P.A.; Chaikin, P.M.; Haddon, R.C. Evidence for Josephson vortices in  $\kappa$ -(BEDT-TTF)<sub>2</sub>Cu(NCS)<sub>2</sub>. *Phys. Rev. B* **1994**, *50*, 15929–15944, doi:10.1103/PhysRevB.50.15929.
61. Singleton, J.; Mielke, C. Quasi-two-dimensional organic superconductors: A review. *Contemp. Phys.* **2002**, *43*, 63–96.
62. Agosta, C.; Martin, C.; Radovan, H.; Palm, E.; Murphy, T.; Tozer, S.; Cooley, J.; Schlueter, J.; Petrovic, C. Penetration depth studies of organic and heavy fermion superconductors in the Pauli paramagnetic limit. *J. Phys. Chem. Solids* **2006**, *67*, 586–589.
63. Coffey, T.; Bayindir, Z.; DeCarolis, J.F.; Bennett, M.; Esper, G.; Agosta, C.C. Measuring radio frequency properties of materials in pulsed magnetic fields with a tunnel diode oscillator. *Rev. Sci. Instr.* **2000**, *71*, 4600–4606, doi:10.1063/1.1321301.
64. Martin, C.; Agosta, C.C.; Tozer, S.W.; Radovan, H.A.; Palm, E.C.; Murphy, T.P.; Sarrao, J.L. Evidence for the Fulde-Ferrell-Larkin-Ovchinnikov state in CeCoIn<sub>5</sub> from penetration depth measurements. *Phys. Rev. B* **2005**, *71*, 020503, doi:10.1103/PhysRevB.71.020503.
65. Martin, C.; Agosta, C.; Tozer, S.; Radovan, H.; Kinoshota, T.; Tokumoto, M. Critical Field and Shubnikov-de Haas Oscillations of  $\kappa$ -(BEDT-TTF)<sub>2</sub>Cu(NCS)<sub>2</sub> under Pressure. *J. Low Temp. Phys.* **2005**, *138*, 1025–1037.
66. Orlando, T.P.; McNiff, E.J., Jr.; Foner, S.; Beasley, M.R. Critical fields, Pauli paramagnetic limiting, and material parameters of Nb<sub>3</sub>Sn and V<sub>3</sub>Si. *Phys. Rev. B* **1979**, *19*, 4545–4561.
67. Schossmann, M.; Carbotte, J. Pauli limiting of the upper critical magnetic field. *Phys. Rev. B* **1989**, *39*, 4210–4216, doi:10.1103/PhysRevB.39.4210.
68. Zuo, F.; Brooks, J.S.; McKenzie, R.H.; Schlueter, J.A.; Williams, J.M. Paramagnetic limiting of the upper critical field of the layered organic superconductor  $\kappa$ -(BEDT-TTF)<sub>2</sub>Cu(SCN)<sub>2</sub>. *Phys. Rev. B* **2000**, *61*, 750–755, doi:10.1103/PhysRevB.61.750.
69. McKenzie, R.H. Wilson's ratio and the spin splitting of magnetic oscillations in quasi-two-dimensional metals. *arXiv* **1999**, arXiv.9905044.
70. Padamsee, H.; Neighbor, J.; Shiffman, C. Quasiparticle phenomenology for thermodynamics of strong-coupling superconductors. *J. Low Temp. Phys.* **1973**, *12*, 387–411.
71. Johnston, D.C. Elaboration of the  $\alpha$ -model derived from the BCS theory of superconductivity. *Superconduct. Sci. Technol.* **2013**, *26*, 115011.
72. Taylor, O.J.; Carrington, A.; Schlueter, J.A. Specific-Heat Measurements of the Gap Structure of the Organic Superconductors  $\kappa$ -(BEDT-TTF)<sub>2</sub>-Cu[N(CN)<sub>2</sub>]Br and  $\kappa$ -(ET)<sub>2</sub>Cu(NCS)<sub>2</sub>. *Phys. Rev. Lett.* **2007**, *99*, 057001, doi:10.1103/PhysRevLett.99.057001.
73. Nakazawa, Y.; Kanoda, K. Low-temperature specific heat of  $\kappa$ -(BEDT-TTF)<sub>2</sub>Cu[N(CN)<sub>2</sub>]Br in the superconducting state. *Phys. Rev. B* **1997**, *55*, R8670–R8673, doi:10.1103/PhysRevB.55.R8670.
74. Analytis, J.G.; Ardavan, A.; Blundell, S.J.; Owen, R.L.; Garman, E.F.; Jeynes, C.; Powell, B.J. Effect of Irradiation-Induced Disorder on the Conductivity and Critical Temperature of the Organic Superconductor  $\kappa$ -(BEDT-TTF)<sub>2</sub>Cu(NCS)<sub>2</sub>. *Phys. Rev. Lett.* **2006**, *96*, 177002, doi:10.1103/PhysRevLett.96.177002.
75. Zantout, K.; Altmeyer, M.; Backes, S.; Valentí, R. Superconductivity in correlated BEDT-TTF molecular conductors: Critical temperatures and gap symmetries. *Phys. Rev. B* **2018**, *97*, 014530, doi:10.1103/PhysRevB.97.014530.
76. Coffey, T.; Martin, C.; Agosta, C.C.; Kinoshota, T.; Tokumoto, M. Bulk two-dimensional Pauli-limited superconductor. *Phys. Rev. B* **2010**, *82*, 212502, doi:10.1103/PhysRevB.82.212502.
77. Mihut, I.; Agosta, C.; Martin, C.; Mielke, C.; Coffey, T. Incoherent Bragg reflection and Fermi-surface hot spots in a quasi-two-dimensional metal. *Phys. Rev. B* **2006**, *73*, 125118, doi:10.1103/PhysRevB.73.125118.

78. Wanka, S.; Hagel, J.; Beckmann, D.; Wosnitza, J.; Schlueter, J.A.; Williams, J.M.; Nixon, P.G.; Winter, R.W.; Gard, G.L. Specific heat and critical fields of the organic superconductor  $\beta''$ -(BEDT-TTF)<sub>2</sub>SF<sub>5</sub>CH<sub>2</sub>CF<sub>2</sub>SO<sub>3</sub>. *Phys. Rev. B* **1998**, *57*, 3084–3088, doi:10.1103/PhysRevB.57.3084.
79. Elsinger, H.; Wosnitza, J.; Wanka, S.; Hagel, J.; Schweitzer, D.; Strunz, W.  $\kappa$ -(BEDT-TTF)<sub>2</sub>-Cu[N(CN)<sub>2</sub>]Br: A Fully Gapped Strong-Coupling Superconductor, *Phys. Rev. Lett.* **2000**, *84*, 6098–6101. doi:10.1103/PhysRevLett.84.6098.
80. Imajo, S.; Kanda, N.; Yamashita, S.; Akutsu, H.; Nakazawa, Y.; Kumagai, H.; Kobayashi, T.; Kawamoto, A. Thermodynamic Evidence of d-Wave Superconductivity of the Organic Superconductor  $\lambda$ -(BETS)<sub>2</sub>GaCl<sub>4</sub>. *J. Phys. Soc. Jpn.* **2016**, *85*, 043705, doi:10.7566/JPSJ.85.043705.
81. Kwok, W.; Welp, U.; Carlson, K.; Crabtree, G.; Vandervoort, K.; Wang, H.; Kini, A.; Williams, J.; Stupka, D.; Montgomery, L. Unusual behavior in the upper critical magnetic fields of the ambient-pressure organic superconductor  $\kappa$ -(BEDT-TTF)<sub>2</sub>Cu[N(CN)<sub>2</sub>]Br [where BEDT-TTF represents bis(ethylenedithio) tetrathiofulvalene]. *Phys. Rev. B* **1990**, *42*, 8686–8689.
82. Mielke, C.; Harrison, N.; Rickel, D.; Lacerda, A.; Vestal, R.; Montgomery, L. Fermi-surface topology of  $\kappa$ -(BEDT-TTF)<sub>2</sub>Cu [N(CN)<sub>2</sub>]Br at ambient pressure. *Phys. Rev. B* **1997**, *56*, 4309–4312.
83. Petrovic, C.; Pagliuso, P.G.; Hundley, M.F.; Movshovich, R.; Sarrao, J.L.; Thompson, J.D.; Fisk, Z.; Monthoux, P. Heavy-fermion superconductivity in CeCoIn<sub>5</sub> at 2.3 K. *J. Phys. Condens. Matter* **2001**, *13*, L337.
84. Ikeda, S.; Shishido, H.; Nakashima, M.; Settai, R.; Aoki, D.; Haga, Y.; Harima, H.; Aoki, Y.; Namiki, T.; Sato, H.; et al. Unconventional Superconductivity in CeCoIn<sub>5</sub> Studied by the Specific Heat and Magnetization Measurements. *J. Phys. Soc. Jpn.* **2001**, *70*, 2248–2251, doi:10.1143/JPSJ.70.2248.
85. Murphy, T.P.; Hall, D.; Palm, E.C.; Tozer, S.W.; Petrovic, C.; Fisk, Z.; Goodrich, R.G.; Pagliuso, P.G.; Sarrao, J.L.; Thompson, J.D. Anomalous superconductivity and field-induced magnetism in CeCoIn<sub>5</sub>. *Phys. Rev. B* **2002**, *65*, doi:10.1103/PhysRevB.65.100514.
86. Abdel-Hafiez, M.; Aswartham, S.; Wurmehl, S.; Grinenko, V.; Hess, C.; Drechsler, S.L.; Johnston, S.; Wolter, A.U.B.; Büchner, B.; Rosner, H.; et al. Publisher's Note: Specific heat and upper critical fields in KFe<sub>2</sub>As<sub>2</sub> single crystals. *Phys. Rev. B* **2012**, *85*, 179901.
87. Hardy, F.; Böhmer, A.E.; Aoki, D.; Burger, P.; Wolf, T.; Schweiss, P.; Heid, R.; Adelman, P.; Yao, Y.X.; Kotliar, G.; et al. Evidence of Strong Correlations and Coherence-Incoherence Crossover in the Iron Pnictide Superconductor KFe<sub>2</sub>As<sub>2</sub>. *Phys. Rev. Lett.* **2013**, *111*, 027002, doi:10.1103/PhysRevLett.111.027002.
88. Zocco, D.A.; Grube, K.; Eilers, F.; Wolf, T.; Löhneysen, H.v. Pauli-Limited Multiband Superconductivity in KFe<sub>2</sub>As<sub>2</sub>. *Phys. Rev. Lett.* **2013**, *111*, 057007, doi:10.1103/PhysRevLett.111.057007.
89. Kim, H.; Tanatar, M.A.; Song, Y.J.; Kwon, Y.S.; Prozorov, R. Nodeless two-gap superconducting state in single crystals of the stoichiometric iron pnictide LiFeAs. *Phys. Rev. B* **2011**, *83*, 100502, doi:10.1103/PhysRevB.83.100502.
90. Cho, K.; Kim, H.; Tanatar, M.; Song, Y.; Kwon, Y.; Coniglio, W.; Agosta, C.; Gurevich, A.; Prozorov, R. Anisotropic upper critical field and possible Fulde-Ferrel-Larkin-Ovchinnikov state in the stoichiometric pnictide superconductor LiFeAs. *Phys. Rev. B* **2011**, *83*, 060502, doi:10.1103/PhysRevB.83.060502.
91. Gruenberg, L.W.; Gunther, L. Fulde-Ferrell Effect in Type-II Superconductors. *Phys. Rev. Lett.* **1966**, *16*, 996–998, doi:10.1103/PhysRevLett.16.996.
92. Singleton, J.; Symington, J.A.; Nam, M.S.; Ardavan, A.; Kurmoo, M.; Day, P. Observation of the Fulde-Ferrell-Larkin-Ovchinnikov state in the quasi-two-dimensional organic superconductor  $\kappa$ -(BEDT-TTF)<sub>2</sub>Cu(NCS)<sub>2</sub> (BEDT-TTF = bis(ethylene-dithio)tetrathiafulvalene). *J. Phys. Condens. Matter* **2000**, *12*, L641–L648.
93. Lortz, R.; Wang, Y.; Demuer, A.; Böttger, P.H.M.; Bergk, B.; Zwicknagl, G.; Nakazawa, Y.; Wosnitza, J. Calorimetric Evidence for a Fulde-Ferrell-Larkin-Ovchinnikov Superconducting State in the Layered Organic Superconductor  $\kappa$ -(BEDT-TTF)<sub>2</sub>Cu(NCS)<sub>2</sub>. *Phys. Rev. Lett.* **2007**, *99*, 187002, doi:10.1103/PhysRevLett.99.187002.
94. Cai, Z.; Wang, Y.; Wu, C. Stable Fulde-Ferrell-Larkin-Ovchinnikov pairing states in two-dimensional and three-dimensional optical lattices. *Phys. Rev. A* **2011**, *83*, 063621.
95. Tokiwa, Y.; Bauer, E.D.; Gegenwart, P. Quasiparticle Entropy in the High-Field Superconducting Phase of CeCoIn<sub>5</sub>. *Phys. Rev. Lett.* **2012**, *109*, 116402.
96. Young, B.L.; Urbano, R.R.; Curro, N.J.; Thompson, J.D.; Sarrao, J.L.; Vorontsov, A.B.; Graf, M.J. Microscopic Evidence for Field-Induced Magnetism in CeCoIn<sub>5</sub>. *Phys. Rev. Lett.* **2007**, *98*, 036402. doi:10.1103/PhysRevLett.98.036402.

97. Kenzelmann, M.; Strässle, T.; Niedermayer, C.; Sigrist, M.; Padmanabhan, B.; Zolliker, M.; Bianchi, A.D.; Movshovich, R.; Bauer, E.D.; Sarrao, J.L.; et al. Coupled Superconducting and Magnetic Order in CeCoIn<sub>5</sub>. *Science* **2008**, *321*, 1652–1654, doi:10.1126/science.1161818.
98. Kenzelmann, M.; Gerber, S.; Egetenmeyer, N.; Gavilano, J.L.; Strässle, T.; Bianchi, A.D.; Ressouche, E.; Movshovich, R.; Bauer, E.D.; Sarrao, J.L.; et al. Evidence for a Magnetically Driven Superconducting Q Phase of CeCoIn<sub>5</sub>. *Phys. Rev. Lett.* **2010**, *104*, 127001, doi:10.1103/PhysRevLett.104.127001.
99. Raymond, S.; Ramos, S.M.; Aoki, D.; Knebel, G.; Mineev, V.P.; Lapertot, G. Magnetic Order in Ce 0.95Nd 0.05CoIn 5: The Q-Phase at Zero Magnetic Field. *J. Phys. Soc. Jpn.* **2014**, *83*, 013707, doi:10.7566/JPSJ.83.013707.
100. Koutroulakis, G.; Stewart, M.D.J.; Mitrovic, V.F.; Horvatic, M.; Berthier, C.; Lapertot, G.; Flouquet, J. Field Evolution of Coexisting Superconducting and Magnetic Orders in CeCoIn<sub>5</sub>. *Phys. Rev. Lett.* **2010**, *104*, 087001, doi:10.1103/PhysRevLett.104.087001.
101. Kumagai, K.; Shishido, H.; Shibauchi, T.; Matsuda, Y. Evolution of Paramagnetic Quasiparticle Excitations Emerged in the High-Field Superconducting Phase of CeCoIn<sub>5</sub>. *Phys. Rev. Lett.* **2011**, *106*, 137004, doi:10.1103/PhysRevLett.106.137004.
102. Hatakeyama, Y.; Ikeda, R. Antiferromagnetic order oriented by Fulde-Ferrell-Larkin-Ovchinnikov superconducting order. *Phys. Rev. B* **2015**, *91*, 094504, doi:10.1103/physrevb.91.094504.
103. Fortune, N.A.; Hannahs, S.T. Top-loading small-sample calorimeters for measurements as a function of magnetic field angle. *J. Phys. Conf. Ser.* **2014**, *568*, 032008, doi:10.1088/1742-6596/568/3/032008.
104. Kim, D.Y.; Lin, S.Z.; Weickert, F.; Kenzelmann, M.; Bauer, E.D.; Ronning, F.; Thompson, J.D.; Movshovich, R. Intertwined Orders in Heavy-Fermion Superconductor CeCoIn<sub>5</sub>. *Phys. Rev. X* **2016**, *6*, 041059, doi:10.1103/PhysRevX.6.041059.
105. Ptok, A.; Crivelli, D. The Fulde-Ferrell-Larkin-Ovchinnikov State in Pnictides. *J. Low Temp. Phys.* **2013**, *172*, 226–233, doi:10.1007/s10909-013-0871-0.
106. Ptok, A. Multiple phase transitions in Pauli-limited iron-based superconductors. *J. Phys. Condens. Matter* **2015**, *27*, 482001, doi:10.1088/0953-8984/27/48/482001.
107. Cho, C.W.; Yang, J.H.; Yuan, N.F.Q.; Shen, J.; Wolf, T.; Lortz, R. Thermodynamic Evidence for the Fulde-Ferrell-Larkin-Ovchinnikov State in the KFe<sub>2</sub>As<sub>2</sub> Superconductor. *Phys. Rev. Lett.* **2017**, *119*, 593–595, doi:10.1103/PhysRevLett.119.217002.
108. Kittaka, S.; Aoki, Y.; Kase, N.; Sakakibara, T.; Saito, T.; Fukazawa, H.; Kohori, Y.; Kihou, K.; Lee, C.H.; Iyo, A.; et al. Thermodynamic Study of Nodal Structure and Multiband Superconductivity of KFe<sub>2</sub>As<sub>2</sub>. *J. Phys. Soc. Jpn.* **2014**, *83*, 013704, doi:10.7566/JPSJ.83.013704.
109. Poole, C.; Farach, H.; Creswick, R.; Prozorov, R. *Superconductivity*; Elsevier Science: New York, NY, USA, 2014.
110. Buzdin, A.I.; Fiz, V.T. Phase diagrams of electronic and superconducting transitions to soliton lattice states. *Sov. Phys. JETP* **1983**, *58*, 428, doi:10.1007/BF02880301.
111. Lebed, A.G.; Wu, S. Larkin-Ovchinnikov-Fulde-Ferrell phase in the superconductor (TMTSF)<sub>2</sub>ClO<sub>4</sub>: Theory versus experiment. *Phys. Rev. B* **2010**, *82*, 172504, doi:10.1103/PhysRevB.82.172504.
112. Lee, I.J.; Brown, S.E.; Naughton, M.J. Unconventional Superconductivity in a Quasi-One-Dimensional System (TMTSF) 2X. *J. Phys. Soc. Jpn.* **2006**, *75*, 051011, doi:10.1143/JPSJ.75.051011.



© 2018 by the author. Licensee MDPI, Basel, Switzerland. This article is an open access article distributed under the terms and conditions of the Creative Commons Attribution (CC BY) license (<http://creativecommons.org/licenses/by/4.0/>).